

# Monolithic-integrated piezoresistive MEMS accelerometer pressure sensor with glass-silicon-glass sandwich structure

Jian Dong<sup>1</sup> · Zhi-jian Long<sup>1</sup> · Heng Jiang<sup>1</sup> · Li Sun<sup>1</sup>

Received: 12 January 2016 / Accepted: 9 May 2016

© The Author(s) 2016. This article is published with open access at Springerlink.com

**Abstract** A monolithic composite MEMS sensor with sandwich structure is designed, simulated, fabricated and characterized. It consists of a rectangular diaphragm piezoresistive pressure sensor and a double-cantilever-mass piezoresistive accelerometer. The professional MEMS software, Intellisuite 8.5, is used to simulate the performances of the composite sensor. The composite sensor is fabricated on a (100)—silicon wafer by using MEMS bulk-micromachining and anodic bonding technology. One-step wet anisotropic etching process on the backside of the wafer can form the main backside shape of the composite sensor including the mass of accelerometer and the pressure sensing diaphragm. The glass-silicon-glass sandwich structure is formed with  $\alpha$ -Si (amorphous silicon)-glass anodic bonding on the top surface of the wafer and Si-glass anodic bonding at the bottom. The fabricated composite sensor is measured, resulting in 33.0  $\mu$ V/V kPa sensitivity for the 450 kPa-ranged pressure sensor, as well as, 11.2  $\mu$ V/V g sensitivity for the 125 g-ranged accelerometer. The die size of the composite sensor chip is 2.5 mm  $\times$  2.5 mm  $\times$  1.4 mm. The measured results show that the composite sensor is appropriate for the application fields such as automobile, aerospace and environment monitoring.

## 1 Introduction

With the development of silicon micromachining technology, silicon pressure sensors (Crescini et al. 2003; Suja et al.

2015; Kulwant singh et al. 2014; Santosh Kumar and Pant 2015) and accelerometers (Liu et al. 2014; Ravi Sankar and Lahiri 2009; Ravi Sankar et al. 2012; Manuel Engesser et al. 2009) have been well developed and widely used in industrial and commercial applications. Recently, with the market expansion of electronic devices including automobiles, aerospace and portable electronics, great research effects have been motivated again to develop monolithic integrated silicon composite sensors that feature high reliability, low costs and mass fabrication capability (Wang et al. 2011, 2012; Xu et al. 2008; Roozeboom et al. 2013).

This study aims at developing a novel monolithic composite MEMS sensor. The composite sensor integrated a piezoresistive pressure sensor and a piezoresistive accelerometer on one chip. It has a sandwich structure and is fabricated using bulk-micromachining process (Chen et al. 2009) and anodic wafer bonding technology (Liu et al. 2011; San et al. 2013). The accelerometer adopts double-cantilever-mass structure by which double cantilevers can lessen lateral sensitivity in insensitive direction and the mass can enlarge sensitivity in sensitive direction. The pressure sensor has rectangular diaphragm structure. The mass of accelerometer and the pressure-sensing diaphragm of pressure sensor are simultaneously wet anisotropic etched by using only one mask. Anodic bonding technology is used to seal the pressure-reference cavity for the pressure sensor and form the vacuum chamber for free motivation of accelerometer's cantilever-mass. Glass is bonded with the low pressure chemical vapor deposition (LPCVD)  $\alpha$ -Si (amorphous silicon) layer in front side of wafer and with the silicon substrate in back side, respectively, to form sandwich structure. Around bonding areas in front side of wafer, trenches are designed and fabricated to ensure the electrical conduction between the LPCVD  $\alpha$ -Si layer and the silicon substrate, which can protect the piezoresistors from p-n junction break-down during anodic bonding process in front side of wafer.

✉ Jian Dong  
zjutdj@zjut.edu.cn

<sup>1</sup> Key Laboratory of Special Purpose Equipment and Advanced Manufacturing Technology, Ministry of Education, Zhejiang University of Technology, Hangzhou, Zhejiang 310032, China

## 2 Design

### 2.1 Sensor structure and configuration

Figure 1 shows the monolithic composite sensor structure before anodic bonding process which consists of an accelerometer and a pressure sensor. The accelerometer

has double-cantilever-mass structure and the pressure sensor has rectangular sensing diaphragm structure. After one-mask wet anisotropic etching, the accelerometer's rectangular diaphragm with a mass and the pressure sensor's rectangular diaphragm are shaped simultaneously. Then, deep reactive ion etching (DRIE) is used to release the accelerometer's diaphragm and form the suspended

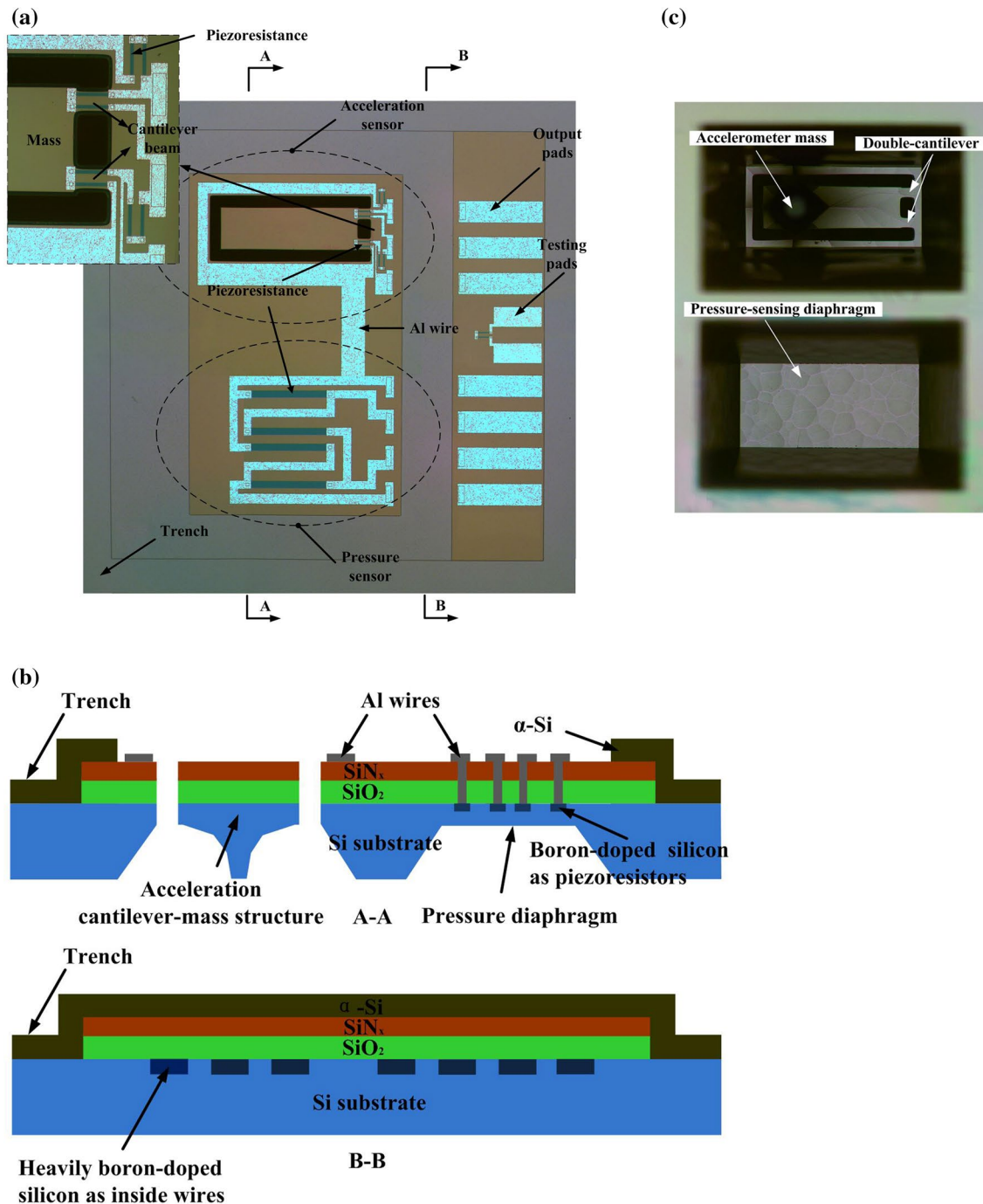


**Fig. 1** The monolithic composite sensor integrated with a piezoresistive accelerometer and a pressure sensor before bonding process: **a** top view; **b** cross section schematic diagram; **c** bottom view

double-cantilever-mass structure. The thickness of accelerometer's diaphragm is designed to be 15  $\mu\text{m}$ , the same as that of the pressure sensor's diaphragm, and the mass of accelerometer is designed to be greatest after wet etching to increase the sensitivity of accelerometer. Boron-doped silicon areas on the substrate work as piezoresistors for both accelerometer and pressure sensor. A layer of thermal-growing  $\text{SiO}_2$  and a layer of LPCVD low-stress  $\text{SiN}_x$  are deposited and patterned on the substrate as passivation layers. Around bonding areas, passivation layers are etched as trenches which expose silicon. A layer of 1  $\mu\text{m}$ -thick LPCVD  $\alpha\text{-Si}$  is deposited and patterned subsequently to connect the silicon substrate by the exposed silicon in trenches, which can help to protect piezoresistors from p-n junction break-down during the  $\alpha\text{-Si}$ -glass anodic bonding process on the top surface. To ensure the bonding strength and airtightness, instead of Al wires, heavily boron-doped

silicon areas are buried beneath the  $\text{SiO}_2/\text{SiN}_x$  passivation layers to electrically connect Al wires with Al pads. The glass-silicon-glass sandwich structure (Roylance and Angell 1979; Zhang et al. 2013) is formed with  $\alpha\text{-Si}$ -glass anodic bonding on the top surface and Si-glass anodic bonding at the bottom, as is shown in Fig. 2.

### 2.2 Design of pressure sensor

Dimensional parameters of the pressure-sensing diaphragm and piezoresistors are shown in Fig. 3. The pressure-sensing diaphragm (Santosh Kumar and Pant 2014, 2016; Bae et al. 2004; Kanda and Yasukawa 1997) is designed to be 950  $\mu\text{m} \times 450 \mu\text{m} \times 15 \mu\text{m}$ , which features high mechanical linearity under 450-kPa ranged pressures. Four boron-doped silicon piezoresistors ( $R_1, R_2, R_3, R_4$ ) are parallelly arranged on edges and the center of the diaphragm along  $\langle 110 \rangle$  direction to form a Wheatstone full-bridge. The piezoresistors are boron-doped to be about  $1 \times 10^{17} \text{cm}^{-3}$  to reduce the temperature effects on sensitivity. The dimensional parameters of the piezoresistors are designed to be 260  $\mu\text{m}$  (length)  $\times$  20  $\mu\text{m}$  (width)  $\times$  3  $\mu\text{m}$  (boron-doping depth).

### 2.3 Design of accelerometer

Dimensional parameters of accelerometer's double-cantilever-mass structure are shown in Fig. 4. Two folded boron-doped silicon piezoresistors ( $R' 1, R' 2$ ) are parallelly arranged on the centers of two cantilevers along  $\langle 110 \rangle$  direction, respectively, and another two ( $R' 3, R' 4$ ) are parallelly arranged on substrate along another direction. Four piezoresistors form a Wheatstone half-bridge with reference resistors  $R' 3$  and  $R' 4$ . The dimensional parameters of the piezoresistors are designed to be 100  $\mu\text{m}$  (length)  $\times$  10  $\mu\text{m}$  (width)  $\times$  3  $\mu\text{m}$  (boron-doping depth). The thickness of accelerometer's diaphragm and cantilevers is designed to be 15  $\mu\text{m}$ , the same as that of the pressure

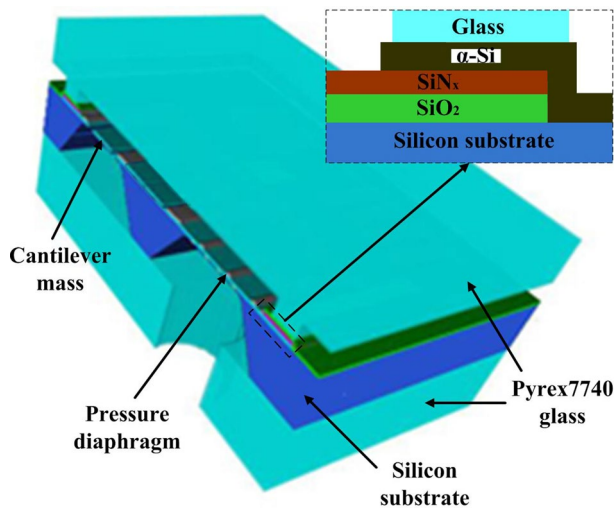


**Fig. 2** 3-D schematic diagram of the sandwich structure with  $\alpha\text{-Si}$ -glass anodic bonding on the top surface and Si-glass anodic bonding at the bottom

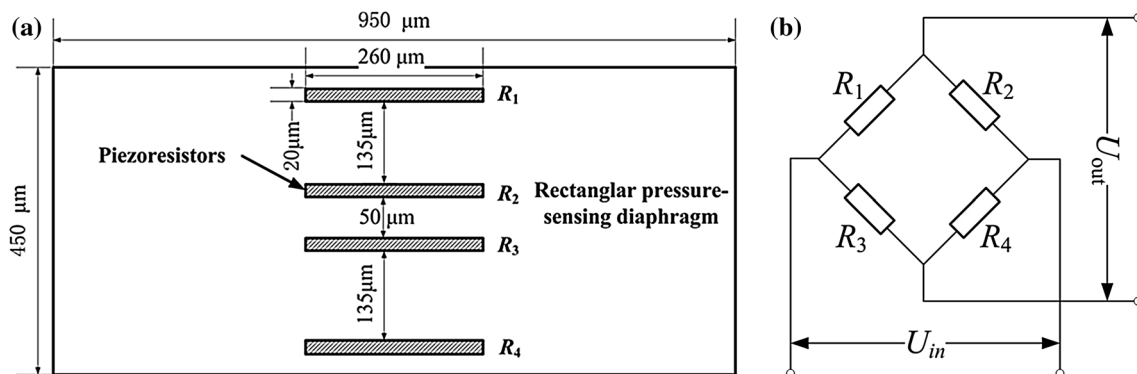


**Fig. 3** a Illustration of the pressure sensor with dimensional parameters, b illustration of the piezoresistors' Wheatstone full-bridge

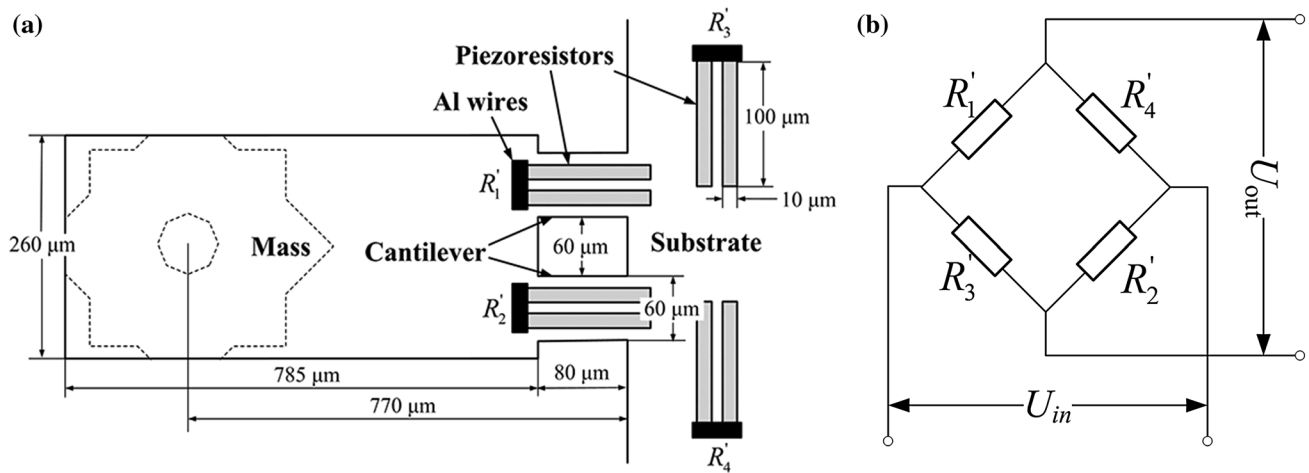


**Fig. 4** **a** Illustration of the double-cantilever-mass structure accelerometer with dimensional parameters; **b** illustration of the piezoresistors' Wheatstone half-bridge ( $R'_3$ ,  $R'_4$  reference resistors)

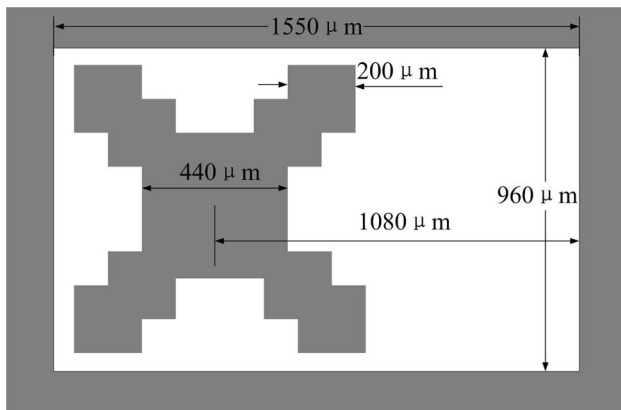


**Fig. 5** The photolithographic mask for anisotropic wet etching of the accelerometer mass

sensor's diaphragm. Two cantilevers are designed to be  $80 \mu\text{m} \times 60 \mu\text{m}$  with the distance of  $60 \mu\text{m}$ . The dimensional parameters of the diaphragm are  $785 \mu\text{m} \times 260 \mu\text{m}$ , and the distance between the center of etched mass and the edge of the substrate is  $770 \mu\text{m}$ .

In order to increase sensitivity, the mass of the accelerometer should be etched to be greatest. The mass is formed by one-mask anisotropic wet etching process and the convex corner compensation etching technique (Fan and Zhang 2006; Offereins 1990; Schroder et al. 2001) is used to design the greatest mass. Because the thickness of silicon substrate is  $380 \mu\text{m}$  and the thickness of accelerometer's diaphragm is  $15 \mu\text{m}$ , the depth of wet etching is calculated to be  $365 \mu\text{m}$ . The mass etching mask design is illustrated in Fig. 5. The dimensional parameters of mask frame are  $1550 \mu\text{m}$  (length)  $\times$   $960 \mu\text{m}$  (width) to ensure

the diaphragm area of  $865 \mu\text{m}$  (length)  $\times$   $260 \mu\text{m}$  (width) after  $365 \mu\text{m}$  depth wet etching process. The center of the big  $440 \mu\text{m}$  side-length square is  $1080 \mu\text{m}$  away from the edge, and eight small  $200 \mu\text{m}$  side-length squares are around four corners of the big square for wet etching compensation. All parameters designed for squares can guarantee the greatest mass after  $365 \mu\text{m}$  depth wet etching process.

### 3 Simulations

The commercial professional MEMS software, Intellisuite 8.5, is used to simulate the performances of the monolithic composite sensor. Intellisuite 8.5 has IntelliEtch module which can demonstrate the etched silicon substrate structure during silicon anisotropic wet etching process, 3D Builder module which can create and mesh a three-dimensional object and TEM module which can perform thermo-electro-mechanical analysis for a multi-conductor electro-mechanical device in multiple physical domains.

#### 3.1 Simulations for pressure sensor

Shown in Fig. 6a, the model of the pressure sensor, which includes a rectangular pressure diaphragm, piezoresistors and wires, is built and meshed by using 3D Builder and then exported to TEM. The material properties of silicon, aluminum and boron-doped silicon (piezoresistor) are listed in Table 1. Figure 6a results show the stress distribution on the pressure diaphragm under  $450 \text{ kPa}$  pressure applied on the top surface. After the stress distribution extracted to electromechanical coupling module,



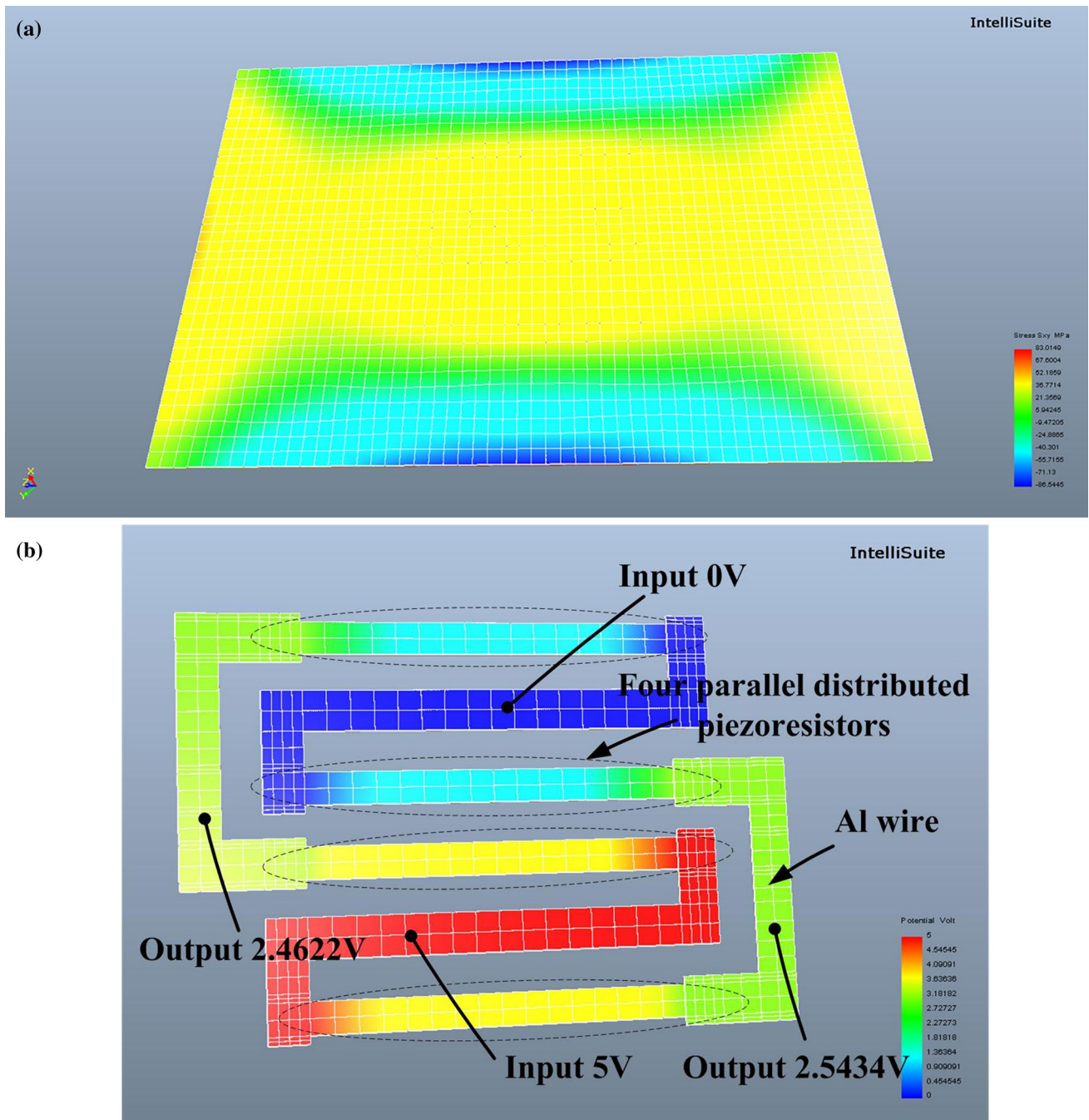


**Fig. 6** Electromechanical coupling simulations of the pressure sensor conducted by TEM: **a** stress distribution on the top surface of the pressure diaphragm under a 450 kPa pressure loaded; **b** electric

potential of four parallel-arranged piezoresistors under a 5 V power supply on the Wheatstone bridge

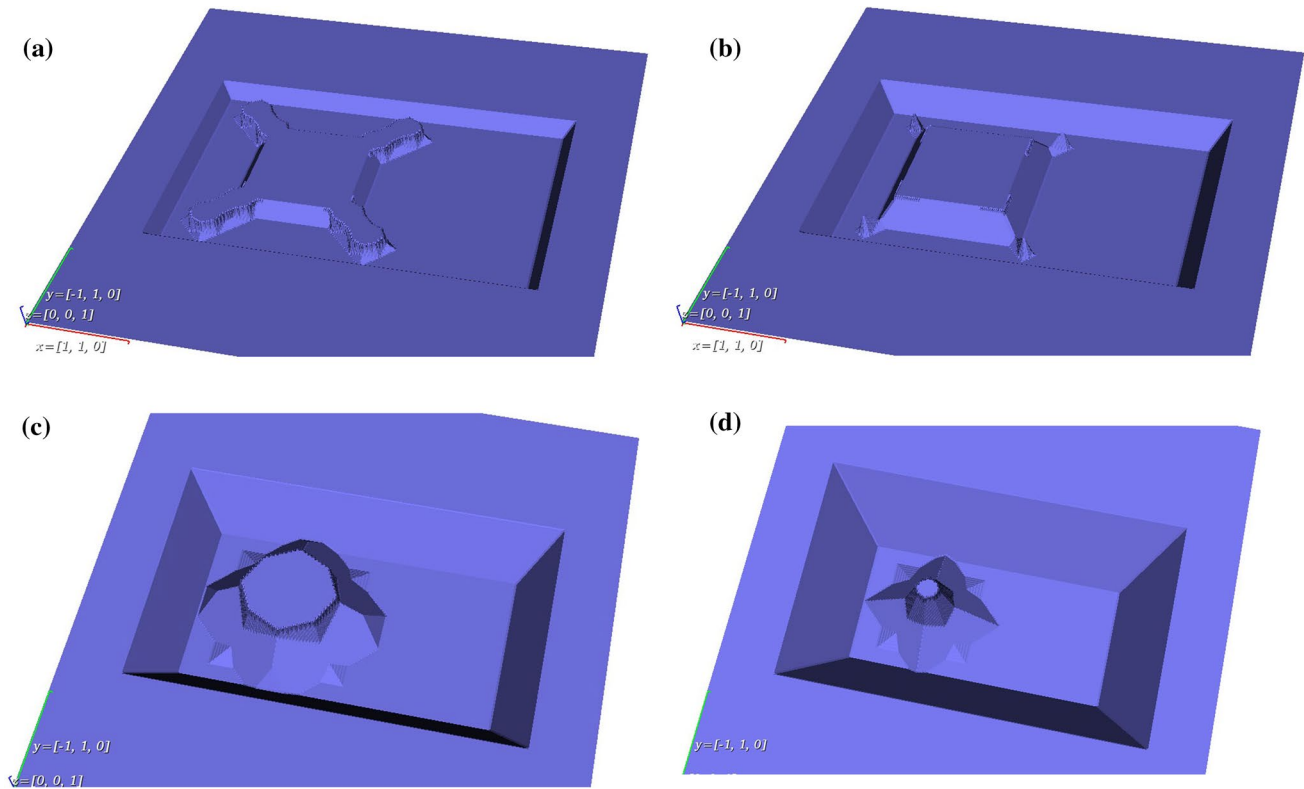
Fig. 6b results show the electric potential distribution of the piezoresistors and wires with a 5 V power supply on the Wheatstone bridge. The output of Wheatstone bridge is  $2.5434 - 2.4622 \text{ V} = 81.2 \text{ mV}$  and the sensitivity of pressure sensor is calculated to be  $81.2 \text{ mV} / (5 \text{ V} \cdot 450 \text{ kPa}) = 36.1 \mu\text{V/V} \cdot \text{kPa}$ .

### 3.2 Simulations for accelerometer

In this design, the mass of the accelerometer is formed using silicon anisotropic wet etching process from the backside of the wafer. To maximize the mass size and get a deeper understanding of etching process, silicon anisotropic wet

**Table 1** Material definition in TEM simulation

Material	Young's modulus (GPa)	Resistivity ( $\Omega$ cm)	Density ( $\text{g}/\text{cm}^3$ )	Piezoresistive coefficient ( $10^{-11}/\text{Pa}$ )
Silicon	168	2.3	2.3	/
Al	74	$4.8 \times 10^{-5}$	2.7	/
P-doped silicon	168	2.3	2.3	$\pi_{11} = 6.6, \pi_{12} = -1.1, \pi_{44} = 138.1$

**Fig. 7** Anisotropic wet etched mass of the accelerometer simulated by IntelliEtch with different etching depths **a** 50  $\mu\text{m}$ ; **b** 110  $\mu\text{m}$ ; **c** 200  $\mu\text{m}$ ; **d** 365  $\mu\text{m}$ 

etching simulation is conducted by IntelliEtch, as is shown in Fig. 7. IntelliEtch module is based on an atomic representation of the anisotropic wet etching dynamic process of silicon substrate, allowing the use of a wide range of Kinetic Monte Carli (KMC) and Cellular Automata (CA) time-evolution (Zhu and Liu 2000; Yan et al. 2008).  $\text{SiO}_2$  and  $\text{SiN}_x$  layers patterned as Fig. 5 are applied on the silicon wafer bottom surface (100) as the etching mask. The anisotropic etch rate of aqueous KOH (45 %, 85 °C) has been calibrated using wagon wheel method (Gosálvez et al. 2011) and is input to the database in software. Figure 8 shows that shapes of accelerometer's mass are formed at different etching depths. Simulation verifies that the etching mask as Fig. 5 can form the greatest mass which is separated to diaphragm edges to be an island.

The accelerometer with double-cantilever-mass structure is modeled according to IntelliEtch simulation results

and subsequently electromechanical coupling simulations are conducted using TEM, as is shown in Fig. 8. Under a 5 V power supply and a 125 g acceleration input, the output of Wheatstone bridge is  $2.5042 - 2.4959 \text{ V} = 8.3 \text{ mV}$ . The sensitivity of accelerometer is calculated to be  $8.3 \text{ mV} / (5 \text{ V} \times 125 \text{ g}) = 13.3 \mu\text{V}/\text{V g}$ .

Vibration modal analysis of accelerometer is also conducted using TEM, which can predict whether the chip is able to work well in a certain noise circumstance. The first vibration mode of the accelerometer is 8.54 kHz, as is shown in Fig. 9.

#### 4 Fabrication

The composite sensor is fabricated with bulk-micromachining process and packaged using anodic wafer bonding

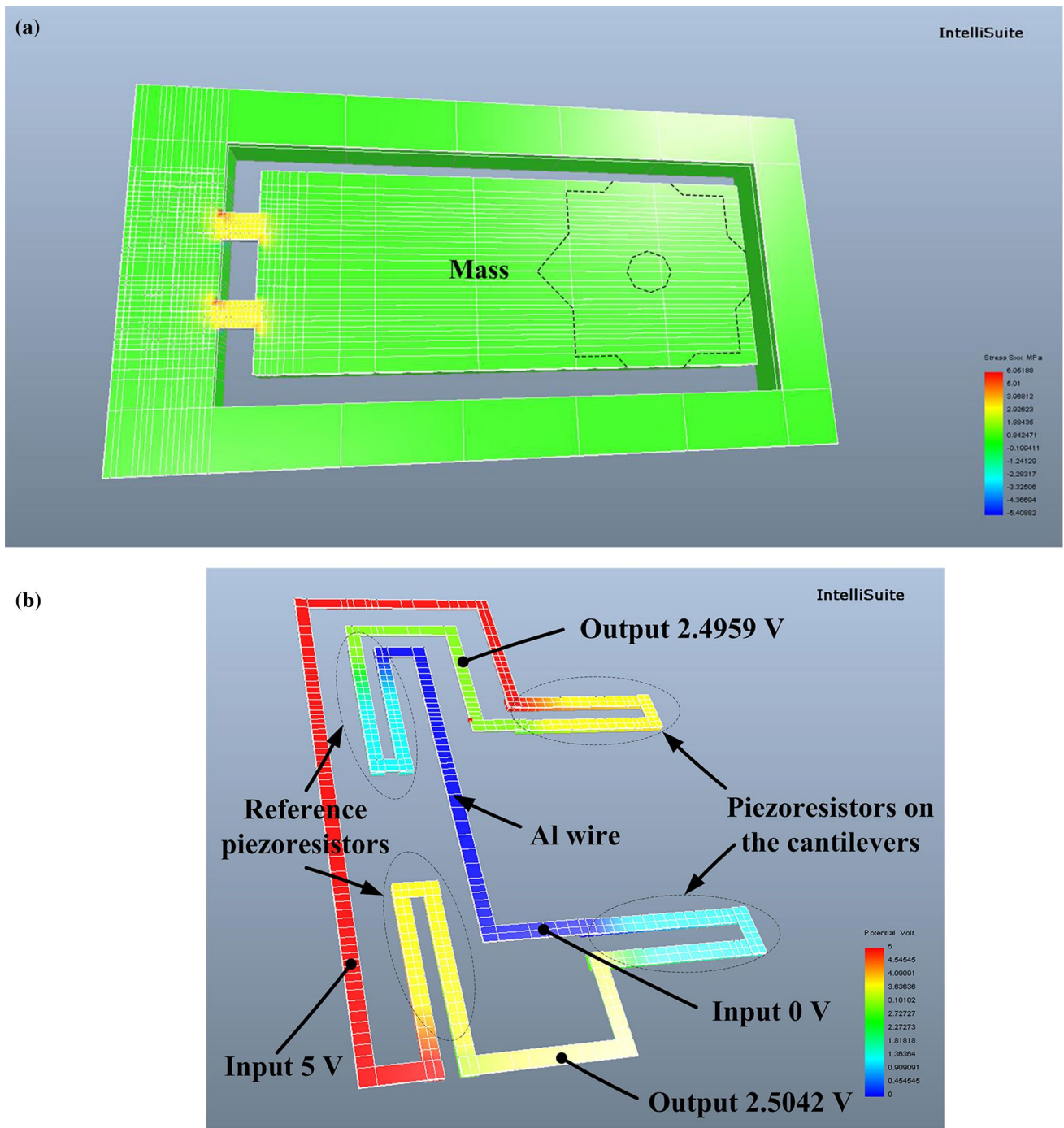


**Fig. 8** Electromechanical coupling simulations of the accelerometer conducted by TEM: **a** stress distribution on the top surface of the double-cantilever-mass structure under a 125 g acceleration loaded;

**b** electric potential of four piezoresistors on the Wheatstone bridge under a 5 V power supply

technology to form a sandwiched structure. Sketched in Fig. 10, fabrication processes start from n-type (100) double-side polished silicon wafer with a resistivity of 5–10  $\Omega$  cm and the thickness of 380  $\mu$ m. The main steps are as follows:

1. Boron is implanted into the substrate and patterned to form piezoresistors of both accelerometer and pressure sensor. Subsequently heavy boron is implanted to form ohmic contact areas in piezoresistors and connecting wires between Al wires and Al pads.

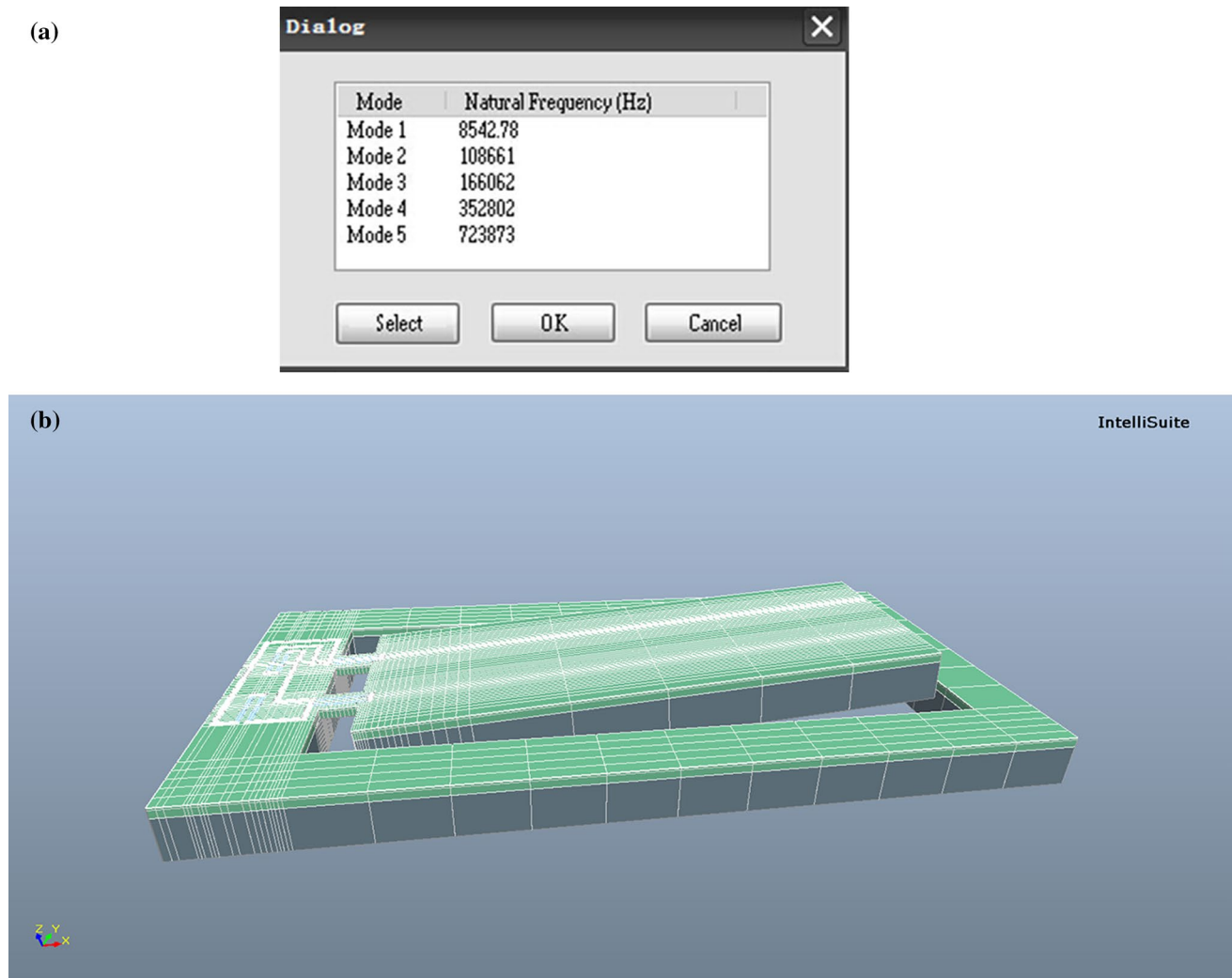


**Fig. 9** Accelerometer vibration mode simulation using TEM: **a** simulation results of the natural frequency from 1st to 5th vibration modes; **b** the first vibration mode of the accelerometer

2. A 0.45  $\mu\text{m}$ -thick thermal-growing  $\text{SiO}_2$  layer and a 0.1  $\mu\text{m}$ -thick LPCVD low-stress (150 MPa)  $\text{SiN}_x$  layer are sequentially deposited on Si wafer and patterned to expose the silicon wafer in trenches. These two layers not only work as passivation and insulating layers for the piezoresistors, but also are used as the hard mask for silicon DRIE.
3. A 1  $\mu\text{m}$ -thick LPCVD  $\alpha\text{-Si}$  layer is deposited on the  $\text{SiO}_2/\text{SiN}_x$  passivation layers and patterned to expose the accelerometer and pressure sensor's working region and the outputpads region.
4. Wire holes are opened on ohmic contact areas by reactive ion etching (RIE). A 1  $\mu\text{m}$ -thick aluminum layer is then magnetron sputtered and patterned for Wheatstone-bridge piezoresistive interconnection and seven output pads.
5. The wafer is soaked into aqueous KOH (45 %, 85 °C) with the clamp protection of the front side of wafer for about 11 h to complete the bottom-release by anisotropic etching. After one-step anisotropic etching, both the accelerometer mass and the pressure sensor diaphragm are formed.
6. The  $\text{SiO}_2/\text{SiN}_x$  layers are drily etched using RIE to expose bare silicon at the bottom surface. The hole-drilled Pyrex7740 glass is bonded to the bottom silicon using anodic bonding with parameters of temperature 350 °C, voltage 800 V, current 20 mA, pressure 1600 N and time 20 min. After bottom bonding, the pressure sensor's sensing diaphragm is exposed to external detected pressure environment by the drilled hole in glass.



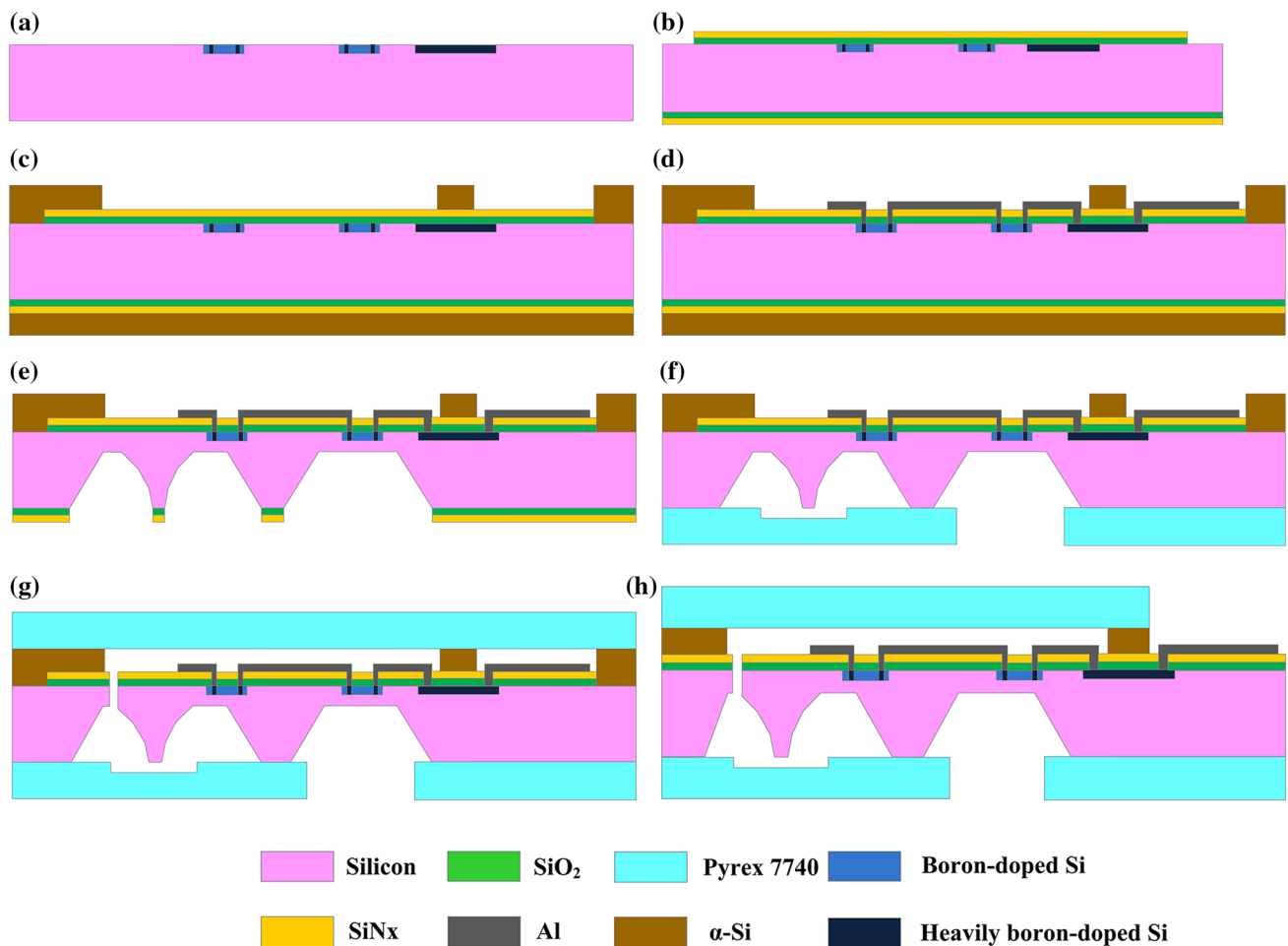


**Fig. 10** Fabrication processes of the monolithic composite sensor, **a** Boron is implanted into the substrate and patterned to form piezoresistors. **b** A 0.45  $\mu\text{m}$ -thick thermal-growing  $\text{SiO}_2$  layer and a 0.1  $\mu\text{m}$ -thick LPCVD low-stress (150 MPa)  $\text{SiN}_x$  layer are deposited and patterned. **c** A 1  $\mu\text{m}$ -thick LPCVD  $\alpha\text{-Si}$  layer is deposited on the  $\text{SiO}_2/\text{SiN}_x$  passivation layers and patterned. **d** Wire holes are opened on ohmic contact areas by reactive ion etching (RIE). **e** The wafer is soaked into aqueous KOH to complete the bottom-release by aniso-

tropic etching. **f** The  $\text{SiO}_2/\text{SiN}_x$  layers are drily etched using RIE to expose bare silicon at bottom. The Pyrex7740 glass is bonded to the bottom using anodic bonding (**g**). The double-cantilever-mass structure is released by DRIE, the Pyrex7740 glass is bonded to the  $\alpha\text{-Si}$  layer at the top surface (**h**). The top glass is diced to have the electric pads exposed. Subsequently, the wafer is saw-diced from the bottom side to form sensor dies

7. The double-cantilever-mass structure is released by DRIE, the Pyrex7740 glass is bonded to the  $\alpha\text{-Si}$  layer at the top surface using anodic bonding with parameters of temperature 400  $^\circ\text{C}$ , voltage 1000 V, current 20 mA, pressure 1600 N and time 20 min. After top bonding, the accelerometer and the pressure sensor are sealed in one cavity at the top surface.
8. The top glass is diced to have the electric pads exposed. Subsequently, the wafer is saw-diced from the bottom side to form the monolithic composite sensor dies.

The micrographs in Fig. 1a, c show the formed device chip before bonding from the front and backside, respectively. Figure 11 shows the device chip after bonding and dicing. The sensor die is as small as 2.5 mm  $\times$  2.5 mm  $\times$  1.4 mm.

## 5 Characterizations and results

### 5.1 Pressure sensor

Shown in Fig. 12, the performances of the pressure sensor in the monolithic composite sensor are measured in a temperature-controlled environmental chamber where the temperature can be adjusted from room temperature to 300  $^\circ\text{C}$  and pressure can be adjusted from 0 to 1000 kPa .

Test results are demonstrated in Fig. 13. Figure 13 shows the output voltage versus the pressure of the pressure sensor at 25  $^\circ\text{C}$  under a 5 V DC supply. Within the range of 0–450 kPa, by using fitting-line method the sensitivity of the pressure sensor is calculated to be 33.0  $\mu\text{V}/\text{V kPa}$ .

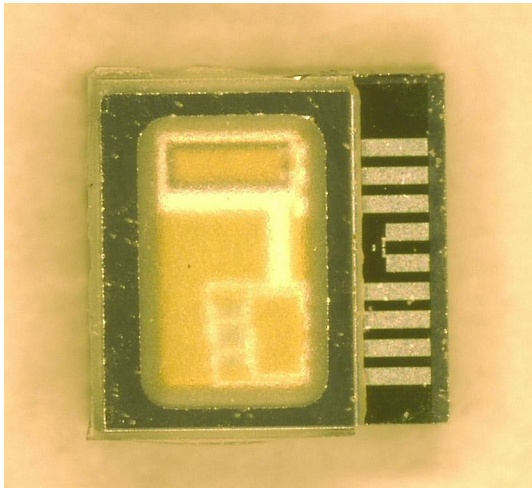


Fig. 11 Micrograph of the device chip after bonding

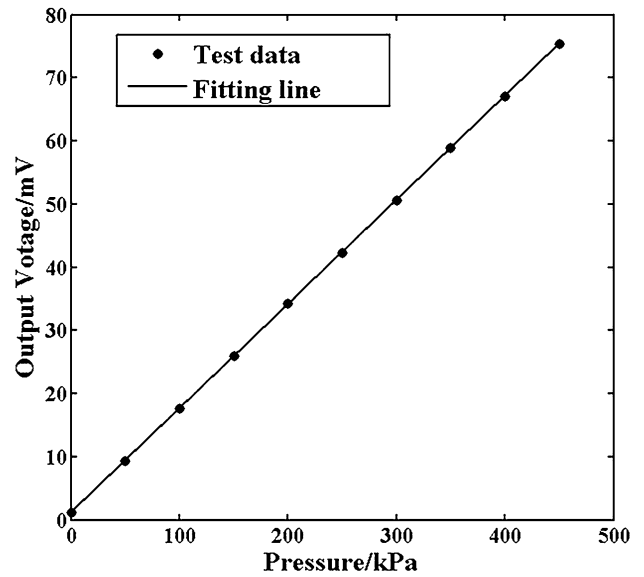


Fig. 13 Voltage output of the pressure sensor in different absolute pressures

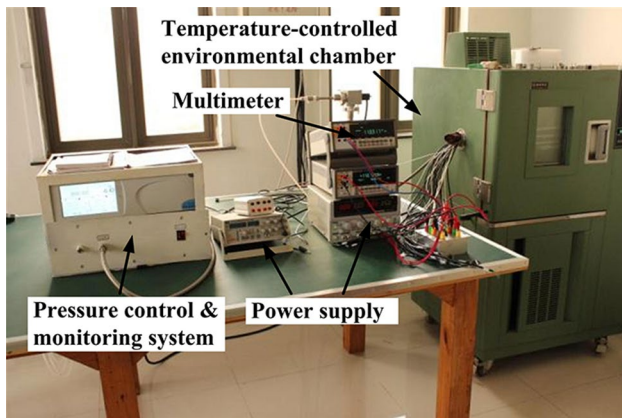


Fig. 12 Measurement setup for the pressure sensor testing

### 5.2 Accelerometer

Shown in Fig. 14, a precise centrifuge turntable and a centrifuge control system are used for the measurement of the accelerometer. To ensure the dynamic balance, two accelerometers are fixed at two edges of the centrifuge turntable. The rotation-generated centrifugal accelerations are adjustable by the centrifuge control system which is controlled by a computer. A DC 5 V power is supplied to the Wheatstone bridge of the accelerometer. The output signal of the accelerometer is directly input a digital multimeter for voltage readout without any amplification.

The output voltage versus the acceleration under a 5 V supply is shown in Fig. 15. Within the measured range of

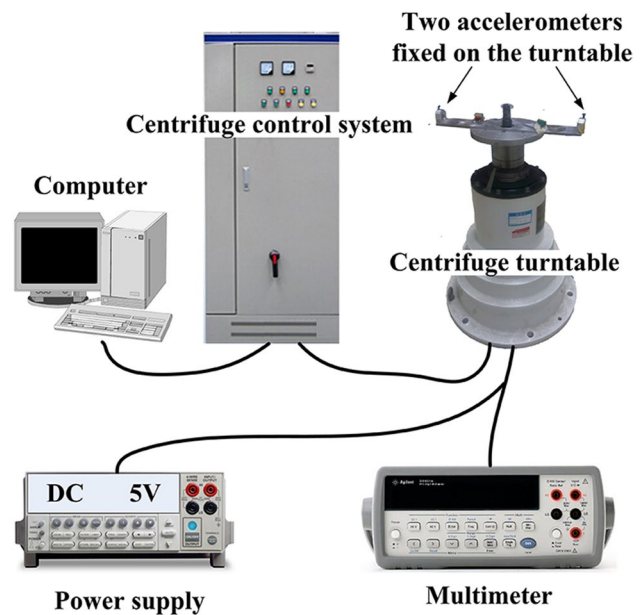


Fig. 14 Schematic diagram of the measurement setup for accelerometer

0–135 g, by using fitting-line method the sensitivity of accelerometer is calculated to be about  $11.2 \mu\text{V/V g}$ . The zero point output of the accelerometer is measured to be 3.81 mV under a 5 V supply.

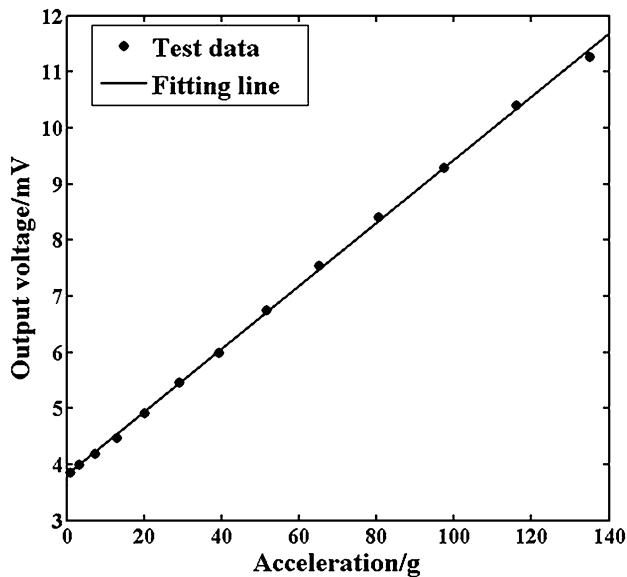


Fig. 15 Voltage output of the accelerometer in different accelerations

## 6 Conclusion

The monolithic composite sensor integrated pressure sensor and accelerometer has been designed and fabricated with compatible bulk-micromachining process and glass-silicon-glass three-layer anodic bonding technique. One-mask anisotropic wet etching from the wafer backside is processed to simultaneously form the pressure sensing diaphragm and the mass of the accelerometer. The composite sensor is packaged by Pyrex7740 glass anodic bonding on both sides of the wafer. On the top side of the wafer, a 1  $\mu\text{m}$ -thick LPCVD  $\alpha\text{-Si}$  layer is deposited to ensure the electrical conduction for anodic bonding and protect the piezoresistors from p-n junction break-down during anodic bonding process. After saw-dicing, this sandwich monolithic composite sensor come to a size of 2.5 mm  $\times$  2.5 mm  $\times$  1.4 mm. Testing results show that the pressure sensor has 33.0  $\mu\text{V/V}$  kPa sensitivity, and the accelerometer has 11.2  $\mu\text{V/V}\cdot\text{g}$  sensitivity. Compared with some piezoresistive accelerometers in literatures or on the market, such as the Infineon SP30T-TPMS products have 8.95  $\mu\text{V/V}$  kPa and 7.74  $\mu\text{V/V}$  g sensitivity, our devised accelerometer exhibits a much increased performance.

Performances of the monolithic composite sensor well meet the requirements of its application fields.

**Acknowledgments** This work is supported by the State Key Laboratories of Transducer Technology Foundation of China under Grant Number SKT1305 and Project of Application Research about Public Welfare Technology in Zhejiang Province under Grant Number 2016C34007. The authors would like to thank the technical staff of the Clean Room Laboratory, Suzhou Institute of Nano-Tech and

Nano-Bionics, Chinese Academy of Sciences, China, for their technical assistance in fabricating the silicon die.

**Open Access** This article is distributed under the terms of the Creative Commons Attribution 4.0 International License (<http://creativecommons.org/licenses/by/4.0/>), which permits unrestricted use, distribution, and reproduction in any medium, provided you give appropriate credit to the original author(s) and the source, provide a link to the Creative Commons license, and indicate if changes were made.

## References

- Bae B, Flachsbarth BR, Park K, Shannon MA (2004) Design optimization of a piezoresistive pressure sensor considering the output signal-to-noise ratio. *J Micromech Microeng* 12:1597–1607
- Chen T, Chen LG, Sun LN, Li XX (2009) Design and fabrication of a four-arm-structure MEMS gripper. *IEEE Trans Ind Electron* 4:996–1004
- Crescini D, Ferrari V, Vajna ZK, Marioli D, Taroni A, Borgese A, Marinelli M, Milani E, Paoletti A, Tucciarone A, Verona-Rinati G (2003) Design and development of a piezoresistive pressure sensor on micromachined silicon for high-temperature applications and of a signal-conditioning electronic circuit. *Microsyst Technol* 9:431–435
- Fan W, Zhang DC (2006) A simple approach to convex corner compensation in anisotropic KOH etching on a (100) silicon wafer. *J Micromech Microeng* 10:1951–1957
- Gosálvez MA, Pal P, Ferrando N, Hida H, Sato K (2011) Experimental procurement of the complete 3D etch rate distribution of Si in anisotropic etchant based on vertically micromachined wagon wheel samples. *J Micromech Microeng* 12:125007–125020
- Kanda Y, Yasukawa A (1997) Optimum design considerations for silicon piezoresistive pressure. *Sens Actuators A* 1:539–542
- Liu J, Shang J, Tang J, Huang QA (2011) Micromachining of Pyrex 7740 glass by silicon molding and vacuum anodic bonding. *J Microelectromech Syst* 4:909–915
- Manuel Engesser, Axel R. Franke, Matthias Maute, Daniel C. Meisel, Jan G. Korvink (2009) Miniaturization limits of piezoresistive MEMS accelerometers. *Microsystem Technologies* 15:1835–1844
- Offereins HL (1990) Methods for the fabrication of convex corners in anisotropic etching of (100) silicon in aqueous KOH. *Sens Actuators A* 1:9–13
- Ravi Sankar A, Lahiri SK (2009) Cross-axis sensitivity reduction of a silicon MEMS piezoresistive accelerometer. *Microsyst Technol* 15:511–518
- Ravi Sankar A, Grace Jency J, Das S (2012) Design, fabrication and testing of a high performance silicon piezoresistive Z-axis accelerometer with proof mass-edge-aligned-flexures. *Microsyst Technol* 18:9–23
- Roozeboom CL, Hopcroft MA, Smith WS, Sim JY (2013) Integrated multifunctional environmental sensors. *J Microelectromech Syst* 3:779–793
- Roylance LM, Angell JB (1979) A batch-fabricated silicon accelerometer. *IEEE T Electron Dev* 12:1911–1917
- San HS, Li Y, Song ZJ, Yu YX, Chen XY (2013) Self-packaging fabrication of silicon-glass-based piezoresistive pressure sensor. *IEEE T Electron Dev* 6:789–791
- Santosh Kumar S, Pant BD (2014) Design principles and considerations for the ‘ideal’ silicon piezoresistive pressure sensor: a focused review. *Microsyst Technol* 20:1213–1247
- Santosh Kumar S, Pant BD (2015) Polysilicon thin film piezoresistive pressure microsensor: design, fabrication and characterization. *Microsyst Technol* 21:1949–1958

- Santosh Kumar S, Ojha Anuj K, Pant BD (2016) Experimental evaluation of sensitivity and non-linearity in polysilicon piezoresistive pressure sensors with different diaphragm sizes. *Microsyst Technol* 22:83–91
- Schroder H, Obermeier E, Horn A, Wachutka GKM (2001) Convex corner undercutting of 100 silicon in anisotropic KOH etching; the new step-flow model of 3-D structuring and first simulation results. *J Microelectromech Syst* 1:88–97
- Singh K, Akhtar J, Varghese S (2014) Multiwalled carb on nanotube-polyimide nano composite for MEMS piezoresistive pressure sensor applications. *Microsyst Technol* 20:2255–2259
- Suja KJ, Kumar GS, Nisanth A, Komaragiri R (2015) Dimension and doping concentration based and performance optimization of a piezoresistive MEMS pressure sensor. *Microsyst Technol* 21:831–839
- Wang Q, Li XX, Li T, Bao MH, Zhou W (2011) On-chip integration of acceleration, pressure and temperature composite sensor with a single-sided micromachining technique. *J Microelectromech Syst* 1:42–52
- Wang JC, Xia XY, Li XX (2012) Monolithic integration of pressure plus acceleration composite TPMS sensors with a single-sided micromachining technology. *J Microelectromech Syst* 2:284–293
- Xu J, Zhao Y, Jiang Z, Sun J (2008) A monolithic silicon multi-sensor for measuring three-axis acceleration, pressure and temperature. *J Mech Sci Technol* 4:731–739
- Yan L, Yulong Z, Bian T, Lu S, Zhongliang Y, Zhuangde J (2014) Analysis and design for piezoresistive accelerometer geometry considering sensitivity, resonant frequency and cross-axis sensitivity. *Microsystem Technologies* 20:463–470
- Yan YD, Sun T, Zhao XS, Hu ZJ, Dong S (2008) Atomistic methods for the simulation of evolving surfaces. *J Micromech Microeng* 5:55029–55045
- Zhang YX, Yang G, Gao CC, Hao YL (2013) A MEMS sandwich differential capacitive silicon-on-insulator accelerometer. *Microsyst Technol* 8:1249–1254
- Zhu ZJ, Liu C (2000) Micromachining process simulation using a continuous cellular automata method. *J Microelectromech Syst* 2:252–261